Journal Pre-proof

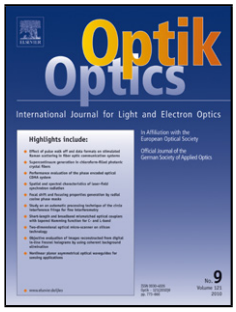

Simulation studies on Polarization modulated Vertical cavity surface emitting laser for combined fiber and free space optical links

K. Murali Krishna, M. Ganesh Madhan, P. Ashok

PII: S0030-4026(20)30854-8

DOI: https://doi.org/10.1016/j.ijleo.2020.165018

Reference: IJLEO 165018

To appear in: *Optik*

Received Date: 15 May 2020

Revised Date: 31 May 2020

Accepted Date: 1 June 2020

Please cite this article as: Krishna KM, Madhan MG, Ashok P, Simulation studies on Polarization modulated Vertical cavity surface emitting laser for combined fiber and free space optical links, *Optik* (2020), doi: https://doi.org/10.1016/j.ijleo.2020.165018

This is a PDF file of an article that has undergone enhancements after acceptance, such as the addition of a cover page and metadata, and formatting for readability, but it is not yet the definitive version of record. This version will undergo additional copyediting, typesetting and review before it is published in its final form, but we are providing this version to give early visibility of the article. Please note that, during the production process, errors may be discovered which could affect the content, and all legal disclaimers that apply to the journal pertain.

© 2020 Published by Elsevier.

Journal Pre-proof

Simulation studies on Polarization modulated Vertical cavity surface emitting laser for combined fiber and free space optical links

K. Murali Krishna[1], M. Ganesh Madhan[2], P. Ashok[3]

[1]Department of Electronics & Communication Engineering, Rajalakshmi Engineering College, Chennai 602105

[2,3]Department of Electronics Engineering, MIT Campus, Anna University, Chennai 600044

Email: [1]muralikrishna.k@rajalakshmi.edu.in, [2]mganesh@annauniv.edu, [3]ashokp2k4@gmail.com

ABSTRACT

In this work, polarization property of Vertical Cavity Surface Emitting Laser (VCSEL) is investigated for 5 Gbps optical data transmission in a combined link comprising of Single Mode Fiber (SMF) and Free Space Optic (FSO) channel. The VCSEL considered for simulation is biased just above threshold with RZ current pulses to emit narrow polarized optical pulses. After 20km SMF link, the received power is launched into two different paths using an optical splitter. It is received by an InGaAs PIN photodiode in one path and a coupling lens in other. A split ratio of 2%, provides the minimum power required for the SMF link to maintain a BER $\leq 10^{-12}$, based on the VCSEL considered in the study. The remaining 98% of power is utilised for FSO transmission beyond the SMF link. The maximum FSO link distances under various loss combinations were found for the two polarised optical pulses, separately. For BER$\leq 10^{-12}$, under the combined influence of all losses, an FSO link length of 130m and 119m, for x and y polarizations are predicted.

KEYWORDS

VCSEL, polarization switching, free space optics, eye diagram, bit error rate, link capacity

Journal Pre-proof

Journal Pre-proof

I. INTRODUCTION

VCSELs are the cost effective, low power laser diodes that find applications in many fields of science and engineering including Gigabit optical data communications. Also, VCSEL's circular cross section aperture and low divergence angle favour Free Space Optics (FSO) based communication links. Integrating dielectric metasurfaces with VCSEL as in [1] for controlling the laser beam profiles, can be used for wide area of applications. For high speed photonics, VCSEL with transverse coupled cavity was modelled with optimized noise characteristics as in [2,3]. A low-oxide aperture diameter VCSEL structure for optical interconnects at 1160 nm was analyzed in [4]. The combo of VCSEL technology and distributed forward amplification aids the transfer of reference frequency clock signal in long reach RF systems, which was demonstrated as in [5]. Theoretical studies with simulation results related to non- linear distortions of polarization hysteresis loop in VCSEL of [6] would help future researchers in developing new optoelectronic systems. The work [7] reports a carrier reservoir splitting approach which accurately explains the intrinsic dynamic characteristics of MM VCSEL. An optimized oxide based aperture VCSEL model was simulated and fabricated in [8], which contributed a low threshold current, high speed and high temperature VCSEL device for various applications. VCSELs were also investigated for Radio over Fiber applications [9,10]. VCSEL along with their polarization properties are familiar in the application of quantum key distribution (QKD) as reported in [11] and in all optical signal processing. Refs. [12-14] reported the polarization dynamics of VCSEL modeling. Yokota et al [15] and Lee et al [16], have explained in their findings how polarization modulation (PM) is best compared with amplitude modulation (AM). According to them, PM, favors the chirp reduction and enhances the performance of switching properties of VCSEL. Hence PM is more efficient for high speed data communication. The effect of polarization and spontaneous noises in VCSEL output power were analyzed by A. Singh et al. [17]. In the trend of FSO based systems, transmitting radio waves with high data rates are inevitable which can be seen in the work of [18], where PDM and OCDMA methods are embarked in Ro-FSO link and system performances were found under various atmospheric conditions. Laguerre Gaussian (LG) modes with gigabit signals were transmitted over free space channel under various climatic conditions in PolSK-MDM-FSO system architecture, as illustrated in [19]. A full-duplex FSO system in [20] with auto locate and fully self align facility was implemented using cost effective commercial components. A new approach was implemented in [21], where multiple photodetector receivers with equal signal

Journal Pre-proof

combiner for improving omnidirectional receiving strength in FSO, was studied. A novel gain switched QCL-FSO-QWIP based communication link was simulated and performances were predicted for OOK, PPM and its variants in [22-28]. In our previous work [29], we employed 1550 nm VCSEL for Hybrid SMF –FSO link, without introducing the polarization effects.

In this work, VCSEL is simulated under two current regions, for which the optical power output exhibits different polarization modes. After reaching threshold, the device lases by means of dominant polarization 'Y' mode and after 5.9 mA [30], polarization switching occurs after which, further increase of current results in increased power output in 'X' mode only. These modes are orthogonal to each other. Such a current based polarization modulation is simulated and utilised for analysing a hybrid SMF-FSO link for 5 Gb/s transmission. The performance is evaluated by calculating the BER and Capacity (b/s/Hz) of the link.

II. STATIC CHARACTERISTICS OF DUAL POLARIZATION VCSEL

Polarization switching (PS) is a phenomenon that exists in VCSEL and not in Edge Emitting Lasers, due to two orthogonally polarised Eigen modes. The circular symmetry of the VCSEL contributes imperfections which decide the magnitude of the two Eigen modes in the light output. When injection current is increased above the threshold, VCSEL lases in one dominant mode while other mode is suppressed. Due to birefringence, there occurs frequency splitting between the two Eigen modes leading to Type I and II PS. When switching takes place from high (Y) to low frequency (X) mode by increasing the injection current, it is said to be Type I PS [30-33] and the opposite mechanism is referred to as Type II PS. Generally, polarization switching depends on injection current and anisotropic properties. Moreover, in the case of external feedback mechanism, the strength and polarization angle also affects the switching. The spin flip model of VCSEL includes coupled rate equations of two linearly polarized fields, (E_x, E_y). Further, carrier rate equation contributes for both sum and difference between population inversions for spin-up and spin-down. Other parameters like cavity field normalized biased current, scaled spontaneous emission rates and fluctuations related to noises are used to obtain laser output power in both polarizations. The below Eqns. (1)-(5) depicts the concept of spin flip model in VCSEL diode adapted from [30].

$$\frac{dE_x}{dt} = -(\kappa + \gamma_a)E_x - i(\kappa\alpha + \gamma_p)E_x + \kappa(1 + i\alpha)(DE_x + inE_y) + \sqrt{\frac{\beta_{sp}\gamma}{2}}(\sqrt{(D+n)}\,\xi_+(t) + \sqrt{(D-n)}\,\xi_-(t)) \qquad (1)$$

Journal Pre-proof

$$\frac{dE_y}{dt} = -(\kappa - \gamma_a)E_y - i(\kappa\alpha - \gamma_p)E_y + \kappa(1+i\alpha)(DE_y - inE_x) + i\sqrt{\frac{\beta_{sp}\gamma}{2}}(\sqrt{(D-n)}\,\xi_-(t) - \sqrt{(D+n)}\,\xi_+(t)) \quad (2)$$

$$\frac{dD}{dt} = -\gamma[D(1+|E_x|^2 + |E_y|^2) - \mu + in(E_y E_x^* - E_x E_y^*)] \quad (3)$$

$$\frac{dn}{dt} = -\gamma_s n - \gamma[n(|E_x|^2 + |E_y|^2) + iD(E_y E_x^* - E_x E_y^*)] \quad (4)$$

Where, $\mu = \frac{\tau_n}{\tau_e}\frac{\frac{I}{I_{th}} - 1}{1 - \frac{N_t}{N_{th}}} + 1$ (5)

Using ode45 MATLAB solver, these interlinked rate equations are evaluated numerically to find laser parameters like polarized fields, spin based sum and differences from population inversions in carriers by employing 4th Order RK method.

From Ref. [30], all the necessary values of laser parameters are taken for solving the rate equations. Figure 1.a shows static characteristics of laser maintained at 25ºC, in which for different bias current, the polarized power obtained from both polarization are mapped correspondingly. The threshold current is found as 1.6 mA and the arbitrary electric field number (no unit) is also plotted in Fig.1b. Fig.1 illustrates polarisation switching behaviour in laser power and E field, for an injection current of 5.9 mA.

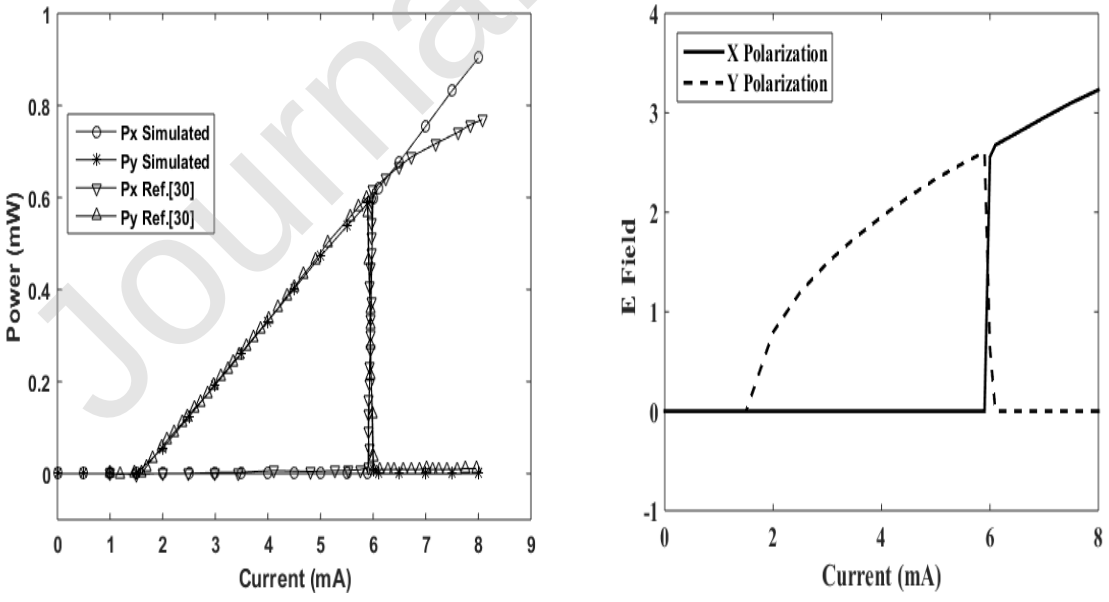

Journal Pre-proof

Journal Pre-proof

(a) **(b)**

Figure 1 (a) Polarization resolved LI Curve (b) Polarization resolved EI Curve

Table I provides the list of VCSEL parameters used in the spin flip rate equation model.

III. TRANSIENT CHARACTERISTICS OF POLARIZATION RESOLVED VCSEL

The current injection and lasing of VCSEL results in x and y polarized output. For achieving stable state of polarization, appropriate magnitude of injection current needs to be selected. For low currents beyond threshold, Y polarization is dominant, while for large pulse amplitude, X polarization is achieved. Figure 2 shows the transient characteristics in VCSEL incorporating polarization switching effect, where Figs. 2.a,c and 2.b,d indicate the input current pulse and output optical power for 3.5mA and 8 mA, respectively. When a 3.5 mA step current pulse given to VCSEL, the output power exhibits an oscillatory behaviour with a peak value of 1.449 mW at high frequency polarization (P_y) with a delay time of 0.56 ns, before settling to a steady value of 0.262 mW. However, the low frequency polarisation output (P_x) is insignificant. Similarly, when a step current of 8 mA is injected to VCSEL, the output power reaches a peak value of 3.517 mW at low frequency polarization (P_x) with a delay time of 0.26 ns and settles to a steady value of 0.90 mW. The high frequency polarisation output (P_y) is suppressed in this case. The transient characteristics of polarisation switching in a different VCSEL laser diode [34], also indicates a similar behaviour, validating our simulation results.

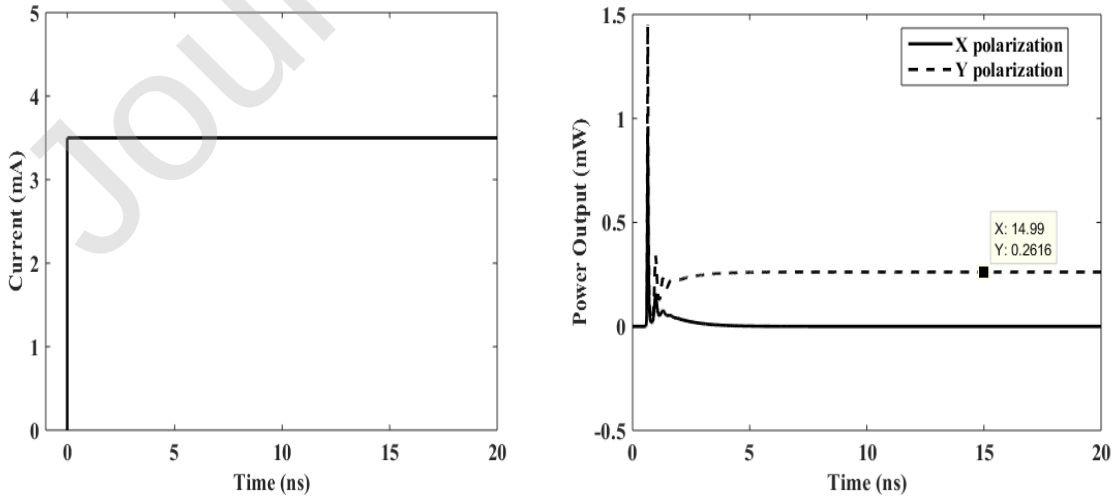

Journal Pre-proof

Journal Pre-proof

(a) **(b)**

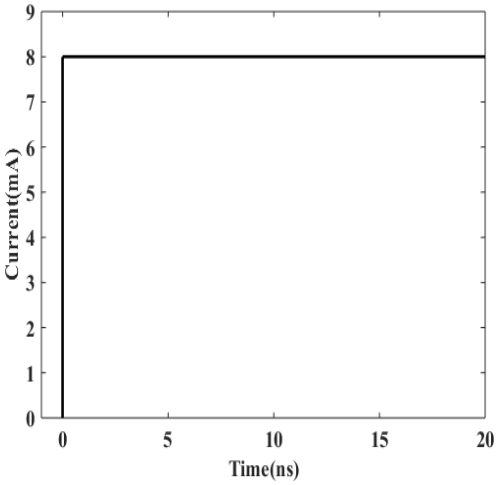

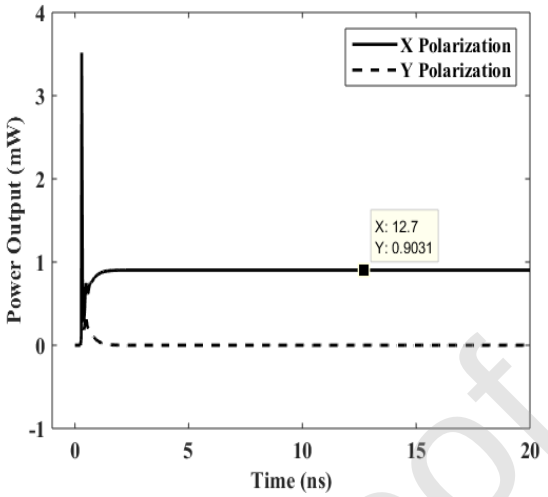

(c) **(d)**

Fig.2.a,c. Input Bias Current respectively. **Fig.2.b,d. Output Laser Power at 3.5 and 8 mA**

IV. BLOCK DIAGRAM OF POLARIZATION RESOLVED VCSEL-SMF-FSO LINK

Figure 3 depicts the complete system model comprising of VCSEL, SMF and FSO blocks mainly. The binary data used in this simulation basically involve 2^7 pseudo random bit combinations. The laser diode is biased with RZ current pulses. Based on the operating current region, one polarization mode is dominant while suppressing the other. The block diagram has been modified with additional polarization controller (PC) and polarization beam splitter (PBS) as in Ref. [35,36], to ensure that one particular polarization alone is transmitted. The receiver remains same as it responds to intensity of the light pulses. With these modifications, the study is focused on the performance of hybrid fiber FSO under these two polarization conditions. The majority of optical power obtained after 20km SMF link is used for FSO transmission through a coupling lens. While the remaining power (2%) is detected using a InGaAs PIN photodiode for data reception. This value indicates the minimum power required in a 20 km SMF link for Passive Optical Network standard to maintain a BER $\leq 10^{-12}$. The coupling ratio is fixed for entire simulation.

Journal Pre-proof

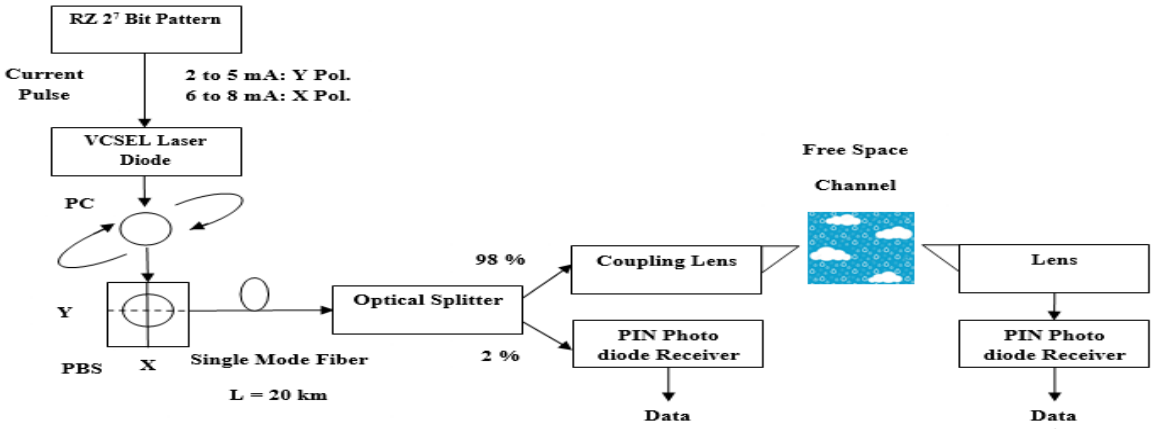

Figure 3 Block diagram of the VCSEL-SMF-FSO based hybrid link.

Table II provides the list of parameters used to model SMF and FSO links for the entire simulation.

V. GIGABIT TRANSMISSION OVER SMF-FSO OPTICAL LINK

The simulation is carried out for each dominant mode separately, by injecting current pulses of appropriate magnitude in to the device.

A. Optical pulse transmission with Y Polarization

For this study, a sequence of 1000 bits which basically involve 2^7 pseudo random bit combinations are taken. VCSEL is operated at 5Gbps of 2.5mA amplitude current pulses following RZ pattern as shown in Fig.4.a. As the polarization beam splitter allows only "Y" polarisation, the power in that mode alone is transmitted through the fiber. The output optical pulses as shown in Fig.4.b are characterised with peak power of 0.63 mW and 26.8 ps of FWHM. The diode detects 2% of the total generated power that is passing through the fiber. The eye diagram plot is shown in Fig. 4.c, from which, the Q factor, BER and capacity are computed. A BER of 6.05×10^{-27} is predicted, which indicates almost zero transmission error and a capacity of 7.84b/s/Hz is obtained using 'Y' polarization in the SMF link.

Journal Pre-proof

Journal Pre-proof

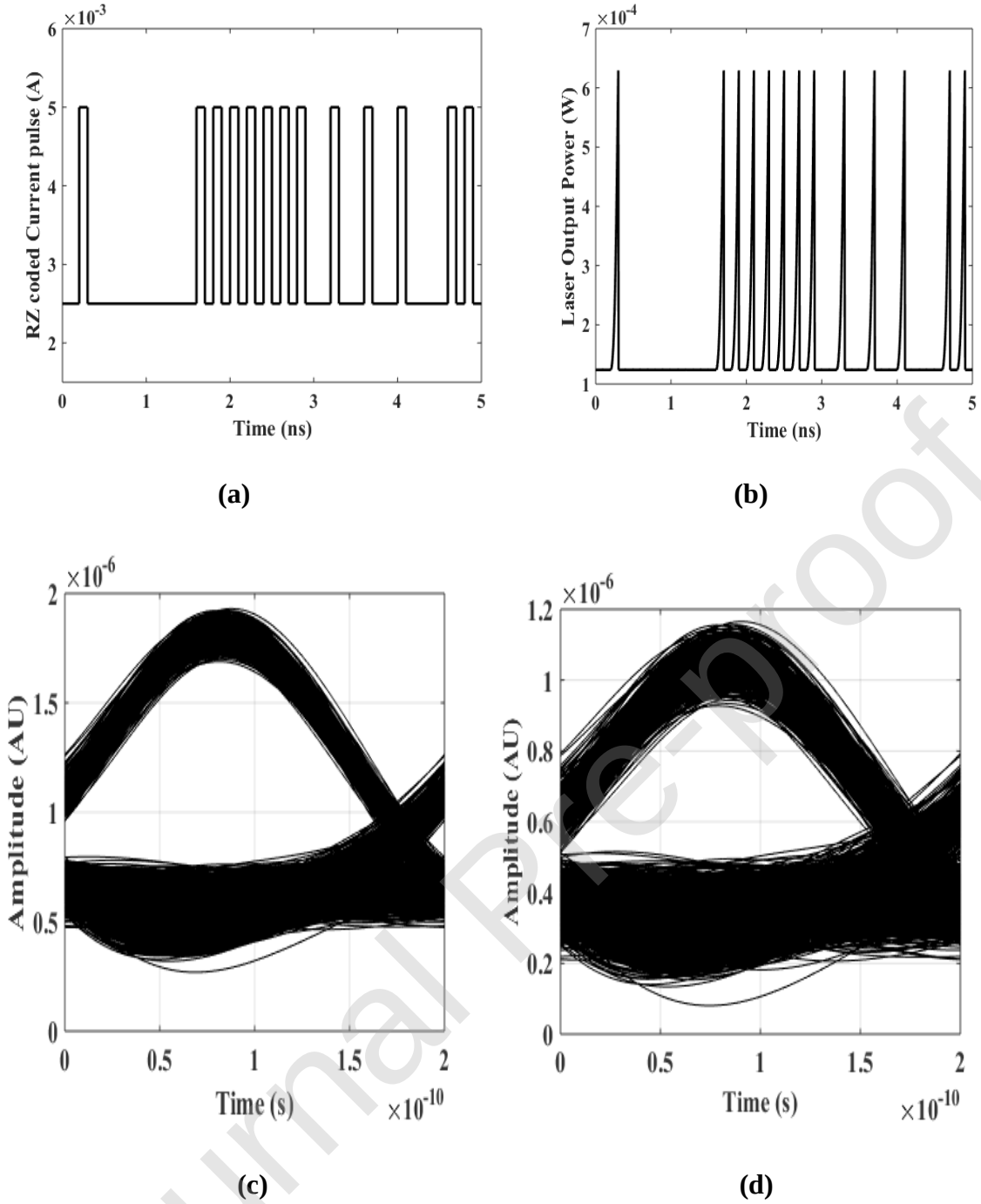

Fig.4 (a) input current sequence (b) output laser power (c) 20 km SMF link eye diagram (d) 530m FSO link eye diagram under Y polarization

A coupling lens receives 98% of the generated power obtained from SMF link and transmit it into free space. The weather condition based attenuation affects FSO channel to a greater extent while its dispersion effects are least significant when comparing with SMF link. The receiver recovers the data from FSO link and Fig.4.d gives the corresponding eye plot. For a BER of 3.1 x 10^{-12} and capacity of 6.58b/s/Hz, the maximum transmission distance is found as

Journal Pre-proof

530m under clear sky condition with an attenuation factor of 0.7 dB/km. The eye diagram of FSO indicates presence of noise, when compared to SMF link.

B. Optical pulse transmission with X Polarization

The procedure carried out for Y polarization is repeated now for X polarization. The output of the polarization beam splitter corresponding to X polarization is connected to the fiber, in this case the diode is biased at 6mA and operated with amplitude of 2mA RZ current pulses as shown in Fig. 5.a. This dc bias value is selected in order to obtain stable 'X' polarization pulses. As shown in Fig.5.b, the laser output has 0.93 mW as peak optical power and 55.3 ps as FWHM. For transmission done using 'X' polarization in the 20km SMF link, the BER and capacity values obtained are 1.31 x 10^{-31} and 8.09 b/s/Hz from eye diagram plot as shown in Fig. 5.c. As in the previous case, the receiver recovers the data from FSO link and Fig.5.d gives the corresponding eye plot with a BER of 4.39 x 10^{-13} and capacity of 6.69 b/s/Hz for a maximum transmission distance of 590m. These values are slightly better than Y polarization, as expected, for clear weather condition. However, if a VCSEL has X polarization above threshold and switches to Y polarization at 6 mA, under similar modulation amplitudes, the results would be the same, as the amplitude of the optical pulses are similar under these conditions.

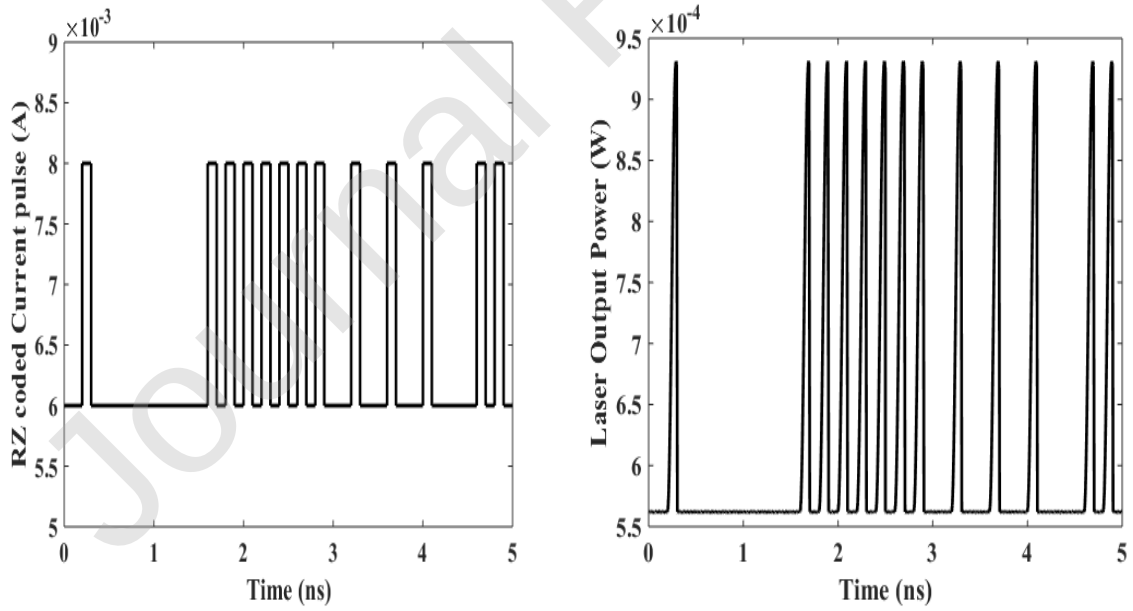

(a) **(b)**

Journal Pre-proof

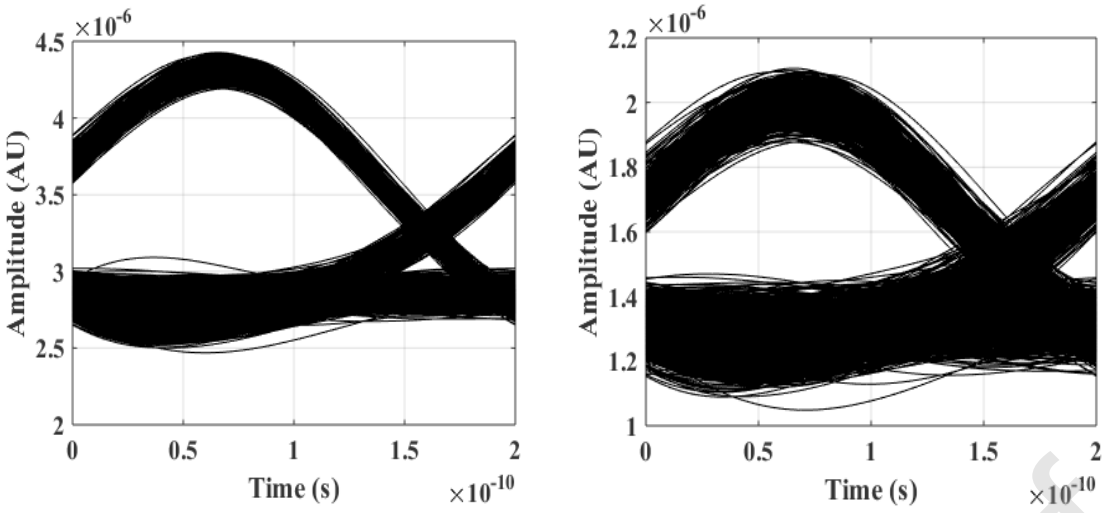

(c) **(d)**

Fig.5 (a) input current sequence (b) output laser power (c) 20 km SMF link eye diagram (d) 590m FSO link eye diagram under X polarization

VI. IMPACT OF VARIOUS LOSSES ON FSO LINK PERFORMANCE

The thorough link analysis of two polarization modes is carried out under FSO losses. Atmospheric loss is characterized by clear weather (0.7 dB/km), light fog (15.96 dB/km) and heavy fog (34.69 dB/km) conditions. Moreover, coupling losses for FSO transmitter or receiver and geometric loss in terms of receiver aperture diameter are also considered in the analysis. FSO distance is varied and the corresponding BER values are calculated from the eye diagram until a maximum BER of 10^{-5} is reached.

A) Effect of atmospheric losses

Under clear weather condition, at BER of 10^{-12}, x and y polarization provide error free transmission upto 596m and 525m respectively. In the presence of light fog, these distances reduce to 338m and 309m, for the same polarizations. The heavy fog condition indicates a maximum transmission distance of 239m and 223m for x and y polarization respectively. All the facts are clearly depicted in Fig. 6.a. Capacity in b/s/Hz also follows a similar trend for clear weather, light and heavy fog conditions, as illustrated in Fig. 6.b.

Journal Pre-proof

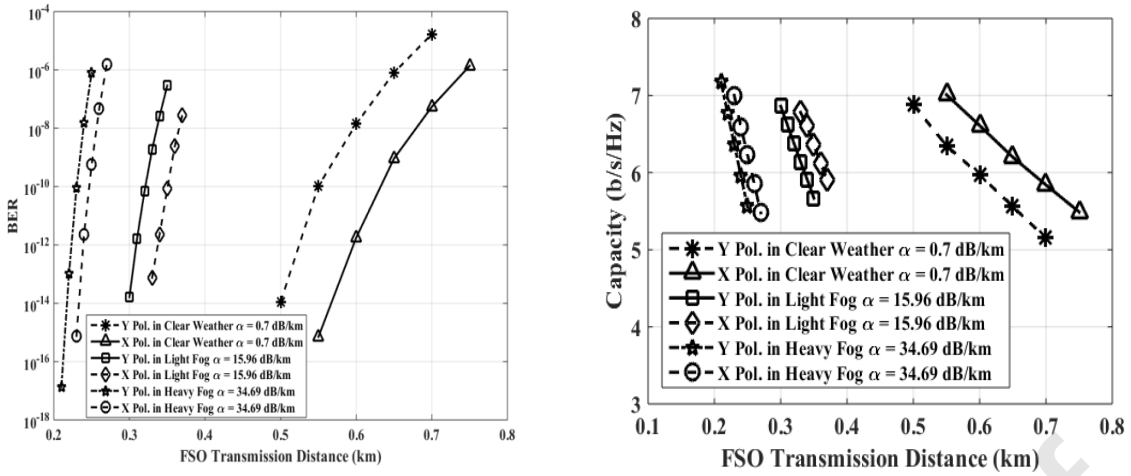

(a) **(b)**

Fig.6(a) BER (b)Capacity Vs FSO transmission distance for clear weather, light and heavy fog conditions using X and Y polarization

B) Effect of Geometric and Coupling losses

In this simulation, geometric loss or coupling loss alone is considered in both x and y polarizations. The distance at which the FSO link achieves a BER of 10^{-12}, is determined. A worst case atmospheric condition (Heavy Fog) with 34.69 dB/km attenuation is also considered for comparison, which provides a maximum link distance of 239m and 223m respectively. The effect of receiver aperture diameter is studied by varying it from 180mm to 90mm [39] and link distances of 304m and 267m, are achieved for error free transmission. Similarly, it is observed that a coupling loss of 10 dB from end to end FSO link, contributes the best performance at a link distance of 429m and 378m for x and y polarization respectively. The performance measure plots shown in Figs.7.a and7.b. The impact of atmospheric loss is more significant when compared to geometric and coupling loss, when considering their effects individually.

Journal Pre-proof

Journal Pre-proof

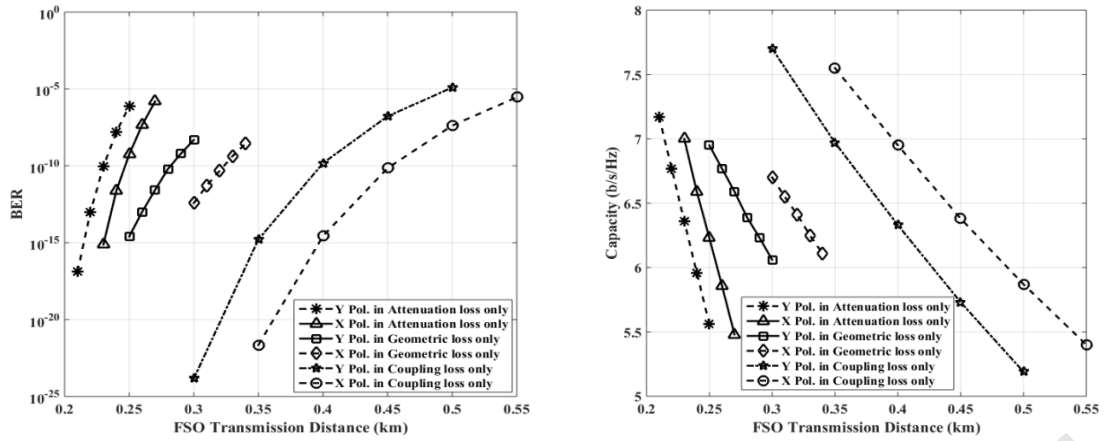

(a) **(b)**

Fig.7(a) BER (b)Capacity Vs Transmission Distance of FSO link under different losses seperately for X and Y polarization

C) Effect of Combined Losses

For a BER = 10^{-12}, the maximum transmission distance possible due to combined effects of coupling and geometric losses are found as 216m and 189m for x and y polarization case. Similarly, when attenuation and coupling losses are combined, the link can produce error free transmission upto 199m and 184m, respectively. It is depicted in Figs. 8.a and 8.b. In the case of combined attenuation and geometric losses, the maximum reach is about 162m and 149m.

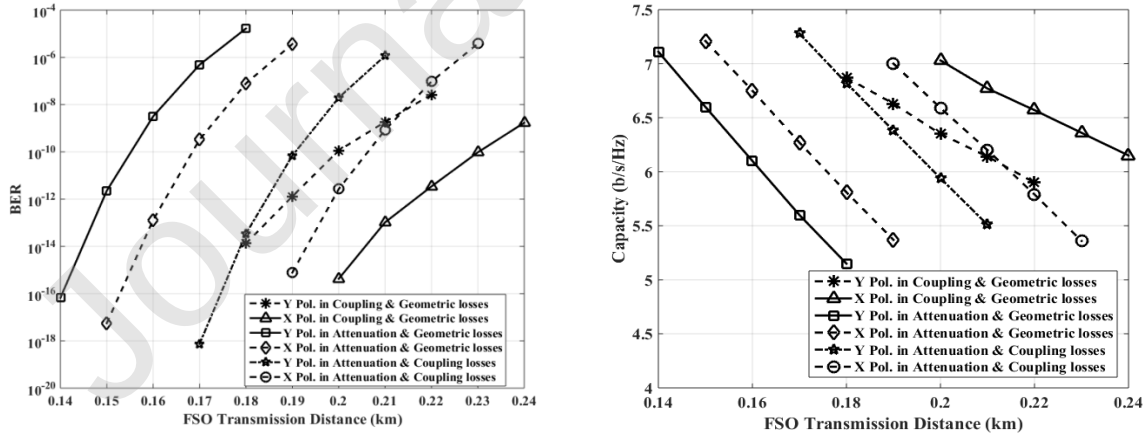

(a) **(b)**

Fig.8(a) BER (b)Capacity Vs Transmission Distance of FSO link under combination of losses for X and Y polarization

Journal Pre-proof

The combined effect of all the three losses under worst case scenario is evaluated, which may severely affect the link performance. A 34.69 dB/km heavy fog, small receiver aperture diameter of 90mm and end-to-end coupling loss of 10 dB are considered. A maximum FSO link distance of 130m and 119m for x and y polarization are achieved for a BER of 10^{-12}. This is less than the other cases, as expected. Both BER and capacity performance are highlighted in Figs. 9.a and 9.b.

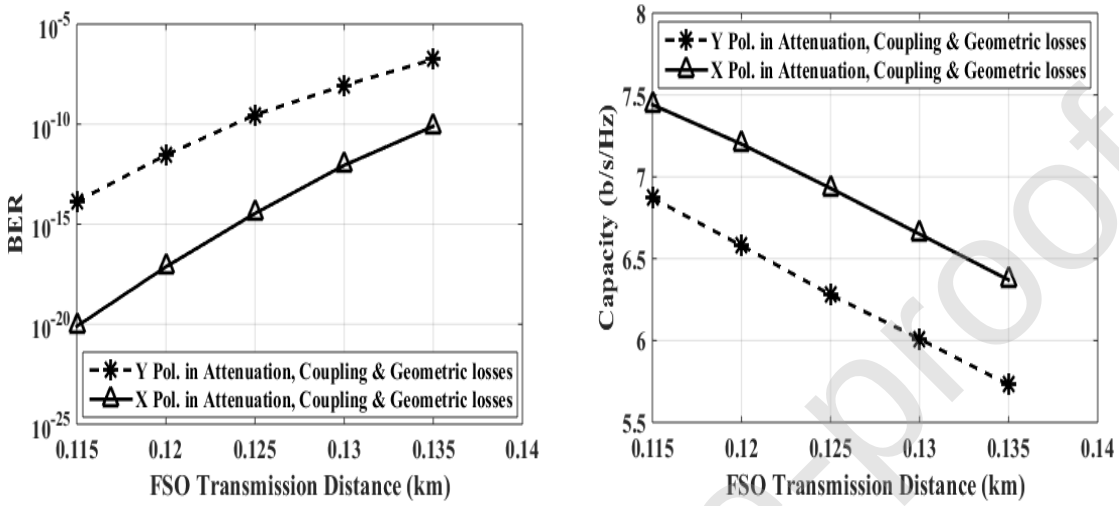

(a) **(b)**

Fig.9(a) BER (b)Capacity Vs Transmission Distance of FSO link under worst case scenario for X and Y polarization.

VII. CONCLUSION AND FUTURE WORK

In the present work, steady state, transient and pulse characteristics of VCSEL are determined by incorporating the polarization properties. From the polarization switching behaviour, it is evident that either polarization P_x (or) P_y contributes for the total power output of the device. A 5 Gbps data transmission for PON application, as well as FSO link extension beyond 20 km SMF, are investigated under individual X or Y polarizations. For a transmission distance of 20 km through SMF, under RZ coding, to achieve a BER of 10^{-12}, 2% of the received power is to found to be sufficient. Remaining 98% is transmitted through free space. The maximum FSO link distances, when considering atmospheric loss alone are found as 239m and 223m, for x and y polarization respectively. A worst case scenario, which includes maximum of all the three losses indicate a transmission distance of 130m and 119m

Journal Pre-proof

for the x and y polarisation modes, beyond the 20 km SMF link. This work can be extended to include polarisation effects in VCSEL for PAM-4 modulation, which is an emerging technique in optical communications.

Declaration of interests

The authors declare that they have no known competing financial interests or personal relationships that could have appeared to influence the work reported in this paper.

REFERENCES

[1]Yi-Yang Xie, Pei-Nan Ni , Qiu-Hua Wang, Qiang Kan , Gauthier Briere, Pei-Pei Chen, Zhuang-Zhuang Zhao, Alexandre Delga, Hao-Ran Ren , Hong-Da Chen, Chen Xu and Patrice Genevet, "Metasurface-integrated vertical cavity surface-emitting lasers for programmable directional lasing emissions", Nature Nanotechnology Volume 15, pp.125-130 (2020).

[2] Hameeda R Ibrahim, Mohamed S Alghamdi, Ahmed Bakry, Moustafa Ahmed and Fumio Koyama, "Modelling and characterisation of the noise characteristics of the vertical cavity surface-emitting lasers subject to slow light feedback", Pramana-J. Phys., Volume 93, pp.1-7 (2019).

[3] M.R.Rajesh Kumar and M.Ganesh Madhan," A comprehensive VHDL – AMS model for a VCSEL based Fiber optic Transmitter", 3rd International Conference on Computers and Devices for Communications (CODEC- 2006), Institute of Radio Physics and Electronics, University of Calcutta, December 18 - 20, 2006.

[4] Priyanka Goyal and Gurjit Kaur, "Design and Analysis of Static Characteristics of VCSEL at 1160 nm for Optical Interconnects", J. Opt. Commun. 0, pp.1-4 (2019).

[5] G. M. Isoe, E. K. Rotich, and T. B. Gibbon," VCSEL-based Raman technology for extended reach time and reference frequency transfer systems", Optoelectronics Letters Volume 15, No. 2, pp.0139-0143 (2019).

[6] M. Jadan, Jihad Addasi, Moayad Husein Flaifel, L.I. Burov, A.S. Gorbatsevich and P.M. Lobatsevich, "The effect of VCSEL intrinsic dynamics on polarization bistability", Results in Physics Voume 14, pp.1-6 (2019).

[7] Marwan Bou Sanayeh, Wissam Hamad and Werner Hofmann," Equivalent Circuit Model of High-Performance VCSELs", Photonics, Volume 7, No.13, pp.1-10 (2020).

[8] Chih-Chiang Shen, Tsung-Chi Hsu, Yen-Wei Yeh, Chieh-Yu Kang, Yun-Ting Lu, Hon-Way Lin, Hsien-Yao Tseng, Yu-Tzu Chen, Cheng-Yuan Chen, Chien-Chung Lin, Chao-Hsin Wu, Po-Tsung Lee, Yang Sheng, Ching-Hsueh Chiu and Hao-Chung Kuo, "Design, Modeling, and Fabrication of High-Speed VCSEL with Data Rate up to 50 Gb/s", Nanoscale Research Letters, Volume 14, No.276, pp. 1-6 (2019).

Journal Pre-proof

Journal Pre-proof

[9] S.Srimathy and M.Ganesh Madhan," Performance Analysis of VCSEL based 2.4 GHz ROF Link ", Photonics 2006, International conference on Photonics and Fiber Optics, University of Hyderabad, Hyderabad, December 13 – 15, 2006.

[10] B.Dhivagar, M.Ganesh Madhan and Xavier Fernando," Analysis of OFDM signal transmission through optical fiber for Radio over fiber transmission", International Workshop on Microwaves and Photonics in Access Networks (MICPAN) 2007, August 21, Ontario, Canada.

[11] Ágoston Schranz and Eszter Udvary, "Polarization Modulated Vertical-Cavity Surface-Emitting Lasers in Quantum Key Distribution", Optics, Photonics and Laser Technology, Volume 223, pp.75-92 (2018).

[12] A. Gahl, S. Balle, and M. San Miguel," Polarization Dynamics of Optically Pumped VCSEL's", IEEE Journal of Quantum Electronics, Vol. 35, No. 3, March 1999, Pages 342-351.

[13] N A Loiko, A V Naumenko and N B Abraham," Complex polarization dynamics in a VCSEL with external polarization-selective feedback", J. Opt. B: Quantum Semiclass. Opt., Vol. 3, 2001, Pages S100–S111.

[14] Ana Quirce, Cristina de Dios, Angel Valle, Luis Pesquera, and Pablo Acedo, "Polarization Dynamics in VCSEL-Based Gain Switching Optical Frequency Combs", Journal of Lightwave Technology, Vol. 36, No. 10, May 15, 2018, Pages 1798-1806.

[15] Nobuhide Yokota, Kunpei Nisaka, Hiroshi Yasaka, and Kazuhiro Ikeda," Spin polarization modulation for high-speed vertical-cavity surface-emitting lasers", Appl. Phys. Lett. 113, 171102, 2018, Pages 1-5.

[16] Jeongsu Lee, William Falls, Rafal Oszwałdowski, and Igor Žutić," Spin modulation in semiconductor lasers", Appl. Phys. Lett. 97, 041116, 2010, Pages 1-3.

[17] A. Singh, M. Sharma and R. Kumar, "Modelling and analysis of polarization noise in vertical cavity surface emitting LASERs", Multiscale and Multidiscip. Model. Exp. and Des. Volume 2, pp.151-157 (2019).

[18] Sushank Chaudhary, Sunita Choudhary, Xuan Tang and Xian Wei, "Empirical Evaluation of High-speed Cost-effective Ro-FSO System by Incorporating OCDMA-PDM Scheme under the Presence of Fog", J. Opt. Commun. 0, pp.1-4 (2020).

[19] Amit Grover, Anu Sheetal and Vigneswaran Dhasarathan," Performance analysis of mode division multiplexing based free space optics system incorporating on–off keying and polarization shift keying under dynamic environmental conditions", Wireless Netw. 0, pp.1-11 (2020).

[20] Mojtaba Mansour Abadi, Mitchell A. Cox, Rakan E. Alsaigh, Shaun Viola, Andrew Forbes and Martin P. J. Lavery, "A space division multiplexed free space-optical communication system that can auto-locate and fully self align with a remote transceiver", Scientific Reports Volume 9, pp.1-8 (2019).

[21] Karel Witas and Jan Nedoma, "Free Space Optic Receiver with Strongly Overlapped Photodetectors' Field of View", Appl. Sci., Volume 9, pp.1-24 (2019).

[22] P. Ashok, M. Ganesh Madhan, "Performance Analysis of Various Pulse Modulation Schemes for a FSO Link Employing Gain Switched Quantum Cascade Lasers", Journal of Optics and Laser Technology, Elsevier Publishing, Volume 111, April 2019, Pages 358-371.

Journal Pre-proof

[23] P. Ashok, M. Ganesh Madhan, "Effect of cold finger temperature on optical pulse modulation characteristics in a 2.59 terahertz quantum cascade laser", Laser Physics Letters, IOP Publishing, Astra Ltd, Volume 17, Number 5, May 2020, Pages 1-7.

[24] P. Ashok, M. Ganesh Madhan, "Numerical analysis on capacity improvement in free space optical link employing two-segment quantum cascade laser-based repeater", Optik - International Journal for Light and Electron Optics, Elsevier Publishing, Vol. 204, 2020, Article No. 164216, pp. 1-7.

[25] P. Ashok, M. Ganesh Madhan, "Effect of Device Parameters on Gain Switching in Quantum Cascade Lasers", Laser Physics Letters, IOP Publishing, Astra Ltd, Volume 16, Number 9, September 2019, Pages 1-6.

[26] P. Ashok, M. Ganesh Madhan, "Particle Swarm Optimization Approach to Identify Optimum Electrical Pulse Characteristics for Efficient Gain Switching in Dual Wavelength Quantum Cascade Lasers", Optik - International Journal for Light and Electron Optics, Elsevier Publishing, Vol. 171, 2018, pp. 786-797.

[27] P. Ashok, M. Ganesh Madhan, "Optimum Electrical Pulse Characteristics for Efficient Gain Switching in QCL", Optik - International Journal for Light and Electron Optics, Elsevier Publishing, Vol. 146C, October 2017, pp. 51-62.

[28] P. Ashok, M. Ganesh Madhan, "Numerical Analysis on the Influence of Device Parameters on the Performance of Quantum Cascade Lasers", Journal of Optoelectronics and Advanced Materials – Rapid Communications, Vol. 10, Iss. 3-4, March - April 2016, pp. 133-142.

[29] K. Murali Krishna and M. Ganesh Madhan, "Vertical cavity surface emitting laser based hybrid fiber-free space optic link for passive optical network applications", Optik - International Journal for Light and Electron Optics, Volume 171, pp.253-265 (2018).

[30] P. Pérez, A. Valle and L. Pesquera," Polarization-resolved characterization of long-wavelength vertical-cavity surface-emitting laser parameters", J. Opt. Soc. Am. B, Vol. 31, Number 11, November 2014, Pages 2574-2580.

[31] Seoung Hun Lee, Hae Won Jung, Kyong Hon Kim and Min Hee Lee," All-optical Flip-flop Operation Based on Polarization Bistability of Conventional-type 1.55-μm Wavelength Single-mode VCSELs", Journal of the Optical Society of Korea, Vol. 14, Number 2, June 2010, Pages 137-141.

[32] A. V. Barve, Y. Zheng, L. Johansson, A. Mehta, A. Husain, and L. Coldren," Ultrafast polarization modulation in vertical cavity surface emitting lasers with frequency dependent current injection", Appl. Phys. Lett.,Vol. 101, Number 251104, December 2012, Pages 1-4.

[33] Dong-Zhou Zhong, Ge-Liang Xu, Wei Luo and Zhen-Zhen Xiao," Reconfigurable dynamic all-optical chaotic logic operations in an optically injected VCSEL", Chin. Phys. B, Vol. 26, No. 12, 2017, 124204 (1-11).

[34] Vijay Manohar Deshmukh, Seoung Hun Lee, Dong Wook Kim, Kyong Hon Kim and Min Hee Lee, "Experimental and numerical analysis on temporal dynamics of polarization switching in an injection-locked 1.55-μm wavelength VCSEL", Optics Express, Volume 19, pp.16934-16949 (2011).

Journal Pre-proof

Journal Pre-proof

[35] P. P´erez, A. Valle, I. Noriega, and L. Pesquera," Measurement of the Intrinsic Parameters of Single-Mode VCSELs", Journal of Lightwave Technology, Vol. 32, No. 8, April 15, 2014, Pages 1601-1607.

[36] Nada Badraoui and · Tibor Berceli," Enhancing capacity of optical links using polarization multiplexing", Optical and Quantum Electronics, Volume 51, No. 310, September 2019. Pages 1-11.

[37] Mazin Ali A. Ali and Emad H. Ahmed, "Performance of FSO Communication System under Various Weather Condition", Advances in Physics Theories and Applications, Volume 43, pp.10-18 (2015).

[38] Koussalya Balasubramanian and Ganesh Madhan, M.,(2009)," Simulation of thermal effects in laser diode and its impact on high speed fiber optic link" International Journal of High speed networks, IOS Press, Netherlands, Vol.17,No.4,pp.175 – 184.

[39] Disha Srivastava, Gurjit Kaur, Garima Singh and Prabhjot Singh, "Evaluation of Atmospheric Detrimental Effects on Free Space Optical Communication System for Delhi Weather",J.Opt. Commun., De Gruyter, pp.1-9 (2020).

Journal Pre-proof

Journal Pre-proof

Table I. VCSEL laser parameters[30]

Parameter	**Value**
minimum active device current, I_{th}	1.602 mA
carrier number at I_{th}, N_{th}	1.21×10^7
carrier lifetime at I_{th}, τ_e	1.21 ns
differential carrier lifetime at I_{th} τ_n	0.48 ns
carrier number when stimulated emission rate equal to the absorption condition, N_t	10.2×10^6
spin flip rate, γ_s	2600 ns^{-1}
linewidth enhancement factor, α	2.8
decay rate of population inversion, γ	2.08 ns^{-1}
field decay rate, κ	33 ns^{-1}
spontaneous emission coefficient, β_{sp}	0.003
linear dichroism, γ_a	dependent on current
linear bifringence, γ_p	95.19 ns^{-1}

Journal Pre-proof

Journal Pre-proof

Table II. Important Parameters used for modelling hybrid SMF-FSO link [29,37].

Parameter	**Value**
Single Mode Fiber	
Insertion loss for split ratio 2/98	1 dB
fiber attenuation factor, α_f	0.2 dB/km
fiber dispersion constant, D	17 ps/nm/km
Free Space Optic link	
FSO coupling loss	[3.5,5] dB
beam divergence, θ	1 mrad
optical efficiency of transmitter, τ_t	0.75
transmitted aperture diameter, D_T	2 mm
optical efficiency of receiver, τ_r	0.75
FSO attenuation factor, α_{FSO}	[0.7,15.96,34.69]dB/km
receiver aperture, D_R	[90,180] mm

The mathematical modeling of SMF, FSO links and photo detector parameters are clearly presented in our earlier work [29]. The received data is extracted using a Butterworth low pass filter of order 4 and 75% of data rate (5 Gbps) [38] as cut off frequency.

Journal Pre-proof